Electrical and dielectric characterization of Au/ZnO/n–Si device depending frequency and voltage

I Orak[1,2], A Kocyigit[3,†], and Ş Alındal[4]

[1] *Bingöl University, Vocational School of Health Services, 12000 Bingöl, Turkey*
[2] *Bingöl University, Faculty of Sciences and Arts, Department of Physics, 12000 Bingöl, Turkey*
[3] *Igdir University, Engineering Faculty, Department of Electrical Electronic Engineering, 76000 Igdir, Turkey*
[4] *Gazi Universty, Faculty of Sciences, Department of Physics, 06500, Ankara, Turkey*

(Received 20 September 2016; revised manuscript received 13 October 2016; published online 10 January 2017)

Au/ZnO/n-type Si device is obtained using atomic layer deposition (ALD) for ZnO layer, and some main electrical parameters are investigated, such as surface/interface state (N_{ss}), barrier height (Φ_b), series resistance (R_s), donor concentration (N_d), and dielectric characterization depending on frequency or voltage. These parameters are acquired by use of impedance spectroscopy measurements at frequencies ranging from 10 kHz to 1 MHz and the direct current (DC) bias voltages in a range from −2 V to +2 V at room temperature are used. The main electrical parameters and dielectric parameters, such as dielectric constant (ε'), dielectric loss (ε''), loss tangent ($\tan\delta$), the real and imaginary parts of electric modulus (M' and M''), and alternating current (AC) electrical conductivity (σ) are affected by changing voltage and frequency. The characterizations show that some main electrical parameters usually decrease with increasing frequency because charge carriers at surface states have not enough time to fallow an external AC signal at high frequencies, and all dielectric parameters strongly depend on the voltage and frequency especially in the depletion and accumulation regions. Consequently, it can be concluded that interfacial polarization and interface charges can easily follow AC signal at low frequencies.

Keywords: Au/ZnO/n–Si device, dielectric properties, polarization process, frequency and voltage dependence

PACS: 81.05.Dz, 85.30.−z, 85.30.Hi, 85.30.Kk **DOI:** 10.1088/1674-1056/26/2/028102

1. Introduction

Metal–semiconductor (or Schottky) devices have been studied largely for years in order to obtain different application areas of these devices, such as low voltage rectifiers, inverters at high frequency, polarity protection and freewheeling diodes.[1–5] In the recent years, they have aroused the researchers' interest in optical and electronic devices.[6–8] For these reasons, these devices should be investigated with different semiconductors or polymers in the interface materials. Already, in this area, researchers investigated new material Schottky devices because they wanted to gain new generation Schottky devices.[9–12] In this respect, here, in the present work, the effect of zinc oxide (ZnO) interfacial layer on electrical and dielectric properties are investigated because it has high direct band gap (3.37 eV), high exciton binding energy (∼ 60 meV), very promising properties like that low costs, non-toxicity and low temperature deposition.[13–16] ZnO also has many application areas such as Schottky barrier diodes (SBDs) solar cells (SCs), chemical sensors (CSs), light-emitting diodes (LEDs), UV and laser diodes (LDs).[17–22]

Dielectric characterization of this device helps to understand conduction and polarization mechanism which can be divided into four parts according to magnitude of applied frequency; electronic, ionic, dipolar, and surface polarizations.[23] Oriental non-dipole polarization usually can be seen in intermediate or high frequency range (10^3 Hz–10^6 Hz) due to long relaxation time (τ). This polarization can be based on existence of constant orientable dipoles, surface charges and impurities.[24] To know more information about polarization and conductions mechanisms, the real and imaginary parts of complex dielectric constant ($\varepsilon^* = \varepsilon' - j\varepsilon''$) and AC electrical conductivity (σ) should be studied in large ranges frequency and voltage. In this way, the more trustworthy and correctly experimental results can be acquired.[25]

There are two main aims in this study: the first one is to best understand the effects of interface states (N_{ss}) or interface traps ($D_{it} = N_{ss}$) with different lifetimes, ZnO interfacial layers, and polarizations on the electrical and dielectric characterization of Au/ZnO/n–Si devices depending on various parameters such as frequency, applied bias voltage, series resistance, interfacial layer, and barrier height (BH) inhomogeneity. The second aim is to fill in this area since dielectric properties of ZnO/n–Si did not studied in literature. Therefore, both the capacitance–voltage (C–V) and conductance–voltage (G/ω–V) measurements of this device is performed in the wide ranges of frequency and voltage at room temperature. The values of ε' and ε'', real and imaginary parts of complex electric modulus ($M^* = M' + jM''$), loss tangent ($\tan\delta$), σ are

†Corresponding author. E-mail: adem.kocyigit@igdir.edu.tr

© 2017 Chinese Physical Society and IOP Publishing Ltd

obtained by using the measured C and G/ω which are dependented on frequency and applied bias voltage.

2. Materials and methods

The n-type Si wafer which was polished and cleaned with various solvents used for fabricating the Au/ZnO/n–Si heterojunction that has (100) orientation and 7.3×10^{15} cm^{-3} donor of concentration atoms. The wafer was degreased consecutively in acetone and methanol for 3 min and then degreased in deionized water with 18 MΩ·cm resistivity at prolonged time. Before formation of ohmic contact, the n-type Si wafer was cut into pieces of 1.0 cm (length) by 1.0 cm (breadth). The degreased wafer was etched with H_2SO_4:H_2O_2:H_2O (5:1:1) for 1 min to remove the surface damages and undesirable impurities. Immediately after surface cleaning, high pure (99.999%) gold with a thickness of 200 nm was thermally evaporated onto the whole back side of the n-Si at about 10^{-6} Torr (1 Torr = 1.33322×10^2 Pa). To form low resistivity back ohmic contact, n-Si/Au structure was annealed at 500 °C for 3 min in N_2 atmosphere. The thickness of metal coverage was determined using a quartz thickness monitor placed in close proximity to the n-Si sample. After forming the ohmic contact, ZnO deposition was achieved by Atomic layer deposition (ALD) technique on n-type Si with Savannah 100 thermal ALD reactor (Cambridge Savannah 100 ALD system) using diethylzinc and water vapor used as zinc and oxygen precursors, respectively and substrate temperature was fixed at 180 °C. The resulting ZnO film growth rate was about 1.45 Å per cycle and final thickness of film was 10 nm. Finally, the Au rectifier/Schottky contacts with 1-mm diameter were formed by evaporating the 200 nm onto the ZnO layer. The (C–V) and (G/ω–V) measurements of the devices were carried out by using an HP 4192 A LF Impedance Analyzer in the wide range of frequency and voltage. All of these measurements were carried out with the help of a microcomputer through an IEEE-488 AC/DC converter card.

3. Results and discussion

It could be understood that the device behaviors are obtained based on the investigations of N_{ss} and R_s because they strongly influence electrical properties.[26] Correlation of N_{ss} with frequency is obtained by Hill–Coleman technique for ZnO/n–Si device. According to this method, the voltage dependence of N_{ss} can be expressed as following relation:[25]

$$N_{ss}=\frac{2}{qA}\frac{(G_m/\omega)_{max}}{((G_m/\omega)_{max}/C_{0x})^2+(1-C_m/C_i)^2}, \quad (1)$$

where A is the Schottky contact area, ω is the angular frequency ($=2\pi f$), C_m is the peak value of capacitance, and $(G_m/\omega)_{max}$ is corresponding to its peak value, C_i is the interfacial insulator layer capacitance obtained from following equation at strong accumulation region[27–29]

$$C_i=C_{ma}\left[1+\frac{G_{ma}^2}{(\omega C_{ma})^2}\right]. \quad (2)$$

Usually, the sources of series resistances (R_s) in electronic devices such as MS, MIS (metal–insulator–semicondcutor) and solar cells are the contact made of the probe wire to the gate, the back contact to the semiconductor, particulate matter between the back contact and the pedestal, the resistance of the quasi-neutral bulk of the semiconductor and an extremely non-uniform doping distribution of donor or acceptor atoms in the semiconductor.[29] On the other hand, the value of shunt resistances (R_{sh}) may originate from a leakage oxide, leakage current paths along the interlayer and shunt paths from the probe wire to the ground. Therefore, to determine the performances and quality of these semiconductor devices, both series and shunt resistances (R_s and R_{sh}) of these devices are very important which are expected to be zero and greater than 10^9 Ω in the ideal case, but the application situation is considerably different from the ideal case. The structure resistance (R_i) is a function of applied bias voltage (V_i), but the real values of R_s for these devices correspond to high enough forward bias voltages or strong accumulation region. The values of R_s for the MS and MIS types become more effective in the high forward bias voltage ($R_i\approx R_s$), leading to a concave curvature or bending of the forward bias C–V plot in an accumulation region. Similarly, the value of R_s also leads to a deviations from linearity in the semi-logarithmic forward bias I–V plots of these devices. In addition, there are many methods in the literature to determine the value of R_s such as Cheung, Norde and Nicollian–Brews methods, but the value of R_s may be different from method to method due to the nature of measured system and applied bias or current range.[27–29] Among these methods, Ohm's law ($R_i=dV_i/dI_i$) and Nicollian–Brews methods are very suitable and reliable to determine R_s values of these devices by using forward bias current–voltage (I–V) and impedance measurement plots (C–V and G/ω–V), respectively, with respect to time consumption, easiness and quickness. In other words, R_i is the structure resistance as a function of applied bias voltage (V_i), but the real values of R_s and R_{sh} for these devices correspond to high enough forward bias voltage or strong accumulation region and low enough reverse bias voltages or strong inversion region, respectively.

The voltage and frequency dependent profile of resistance (R_i) can also be determined from the measured values of capacitance and conductance (C_{mi} and G_{mi}) measurements for each frequency, but the real value of it corresponding to the

strong accumulation region at enough high frequency ($f \geq$ 500 kHz) by using Nicollian and Brews method through using the following relation[29]

$$R_{\rm i}=\frac{G_{\rm mi}}{G_{\rm mi}^2+(\omega C_{\rm mi})^2}. \quad (3)$$

The voltage-dependent $R_{\rm i}$ profiles for various frequencies are shown in Fig. 1. It could be seen in this figure that $R_{\rm i}$ values are constant in the inversion and accumulation region, but there are peaks in depletion region for almost all frequencies. However, intensities of peaks decrease with frequencies increasing from 10 kHz to 1 MHz. This situation could be explained that interface states become effective at low frequencies.

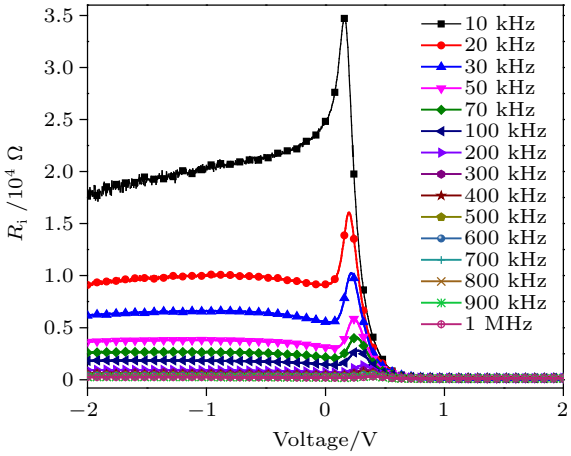


Fig. 1. (color online) Plots of resistance versus voltage for various frequencies.

On the other hand, $R_{\rm i}$ has peaks in the depletion region and peak positions change to forward bias with increasing frequency due to a special density distribution of $N_{\rm ss}$ at ZnO/n–Si and restructure and their reordering under action of electric field.[27,28] The values of $R_{\rm i}$ for high frequencies and forward bias voltages (accumulation region) are almost independent of voltage, and so they are for intermediate and higher frequencies.

In a strong accumulation region ($V \geq 2$ V), the real value of $R_{\rm i}$ correspond to real value of series resistance $R_{\rm s}$, but the maximum value of $R_{\rm i}$ at high reverse bias ($V \leq -2$ V) corresponds to the real value of shunt resistance ($R_{\rm sh}$).[25] $R_{\rm s}$ value is discussed by changing frequency in the next part of this study.

Such frequency and voltage dependence values of $N_{\rm ss}$ and $R_{\rm s}$ are demanded that special attention is paid to their effects in the application of C–V and G/ω–V characteristics. The frequency dependent profiles of $N_{\rm ss}$ and $R_{\rm s}$ (at 2 V) for Au/ZnO/n–Si device are calculated from Eqs. (1) and (3), respectively, and shown in Fig. 2. The values of $N_{\rm ss}$ and $R_{\rm s}$ (at zero and 2 V) changing with frequency are also listed in Table 1. According to the plots of $N_{\rm ss}$ and $R_{\rm s}$ versus frequency of Au/ZnO/n–Si device, they increase at low frequencies, which can be attributed to the fact that they follow alternating current (AC) signal at those frequencies, but at high frequencies, they have decreasing tendency because the charges at traps cannot follow the AC signal.[28]

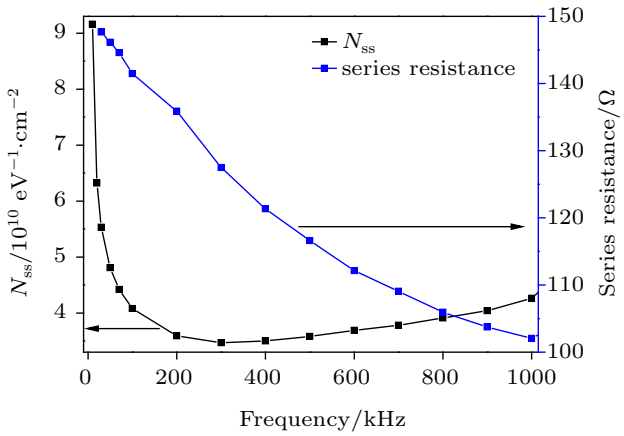


Fig. 2. (color online) Plots of surface state ($N_{\rm ss}$) and series resistance ($R_{\rm s}$) versus frequency of Al/ZnO/n–Si device.

Table 1. Some electrical parameters of Au/ZnO/n–Si device at various frequencies.

f/kHz	$N_{\rm d}$/10^{15} cm^{-3}	$R_{\rm i}$ (at 0 V)/Ω	$R_{\rm s}$ (at 2 V)/Ω	$\Phi_{\rm b}$/eV	$N_{\rm ss}$/10^{10} eV^{-1}· cm^{-2}
10	3.15	2.48×10^4	142.5	2.06	9.16
20	2.97	9.15×10^3	138.2	1.94	6.32
30	2.90	5.54×10^3	147.7	2.17	5.53
50	2.79	3.11×10^3	146.1	2.06	4.81
70	2.73	2.15×10^3	144.6	2.02	4.42
100	2.67	1.47×10^3	141.5	2.02	4.08
200	2.67	7.16×10^2	135.9	1.95	3.59
300	2.48	4.88×10^2	127.5	1.96	3.47
400	2.44	3.78×10^2	121.3	1.93	3.50
500	2.41	3.13×10^2	116.6	1.94	3.58
600	2.39	2.71×10^2	112.1	1.94	3.69
700	2.38	2.41×10^2	109.1	1.98	3.78
800	2.37	2.19×10^2	105.9	1.97	3.91
900	2.37	2.02×10^2	103.7	1.97	4.04
1000	2.37	1.92×10^2	102.1	2.04	4.26

The values of intercept or diffusion potential ($V_d = V_i + kT/q$) and concentration of donor atoms (N_d) are obtained from the intercept and slope of the straight line part of $1/C^{-2}$ versus V plots for all measured frequencies, respectively.[30] The values of barrier height (BH) with changing frequency could be obtained from the following formula:

$$\Phi_b(C-V) = (V_d + E_F) - \Delta\Phi, \tag{4}$$

where E_F is the Fermi energy level and $\Delta\Phi$ is the image force BH lowering obtained from reverse bias C–V measurements, and it is negligibly small for intermediate doping concentration of semiconductor. As shown in Fig. 3, barrier height values generally decrease (first linear) down to 500 kHz then increased (second linear) with increasing frequency, but N_d values decrease with increasing frequency which is attributed to the fact that the electric charges are located in surface states and cannot follow an external AC signal at enough high frequencies. These cases can also be attributed to the particular distribution of N_{ss} and its relaxation time and inhomogeneity of interlayer.[28] The surface and dipole polarization are also more effective on the C–V and G/ω–V characteristics, and so the electric and dielectric properties can be discussed at low and intermediate frequencies.

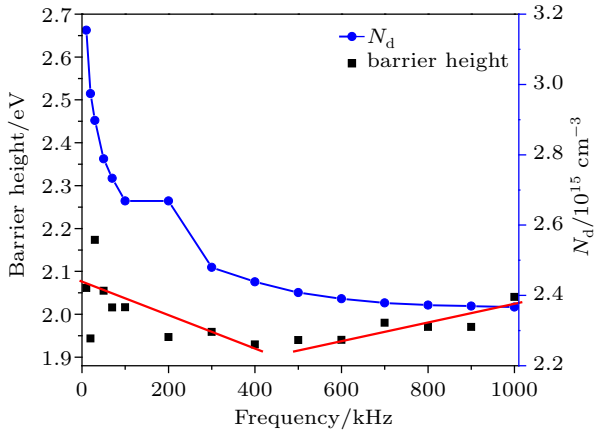


Fig. 3. (color online) Variations of BH and concentration of donor atoms (N_d) with frequency.

The complex permittivity of dielectric material can be obtained from the following relation:

$$\varepsilon^* = \varepsilon' - j\varepsilon'' = \frac{C}{C_0} - j\frac{G}{\omega C_0}, \tag{5}$$

where ε' and ε'' are called sequentially real and imaginary components of complex dielectric constant (ε^*), j is the imaginary root, C and G are the measured real and imaginary component of impedance (Z) or admittance ($Z = 1/Y$), respectively, and C_0 is the capacitance of free capacitor. So, both the values of ε' and ε'' can be determined from the values of C and G by using following relations[24]

$$\varepsilon' = \frac{C}{C_0} = \frac{Cd_i}{\varepsilon_0 A}, \tag{6}$$

$$\varepsilon'' = \frac{G}{\omega C_0} = \frac{Gd_i}{\varepsilon_0 \omega A}. \tag{7}$$

Here, A is the contact area of device, d_i is the thickness of interlayer, and ε_0 is the permittivity of vacuum. Maximum capacitance value at enough high forward biases is corresponding to interlayer capacitance, and written as $C_{ac} = C_i = \varepsilon'\varepsilon_0 A/d_i$. The loss tangent ($\tan\delta$) can be given as follows:

$$\tan\delta = \frac{\varepsilon'}{\varepsilon''} = \frac{G}{\omega C}. \tag{8}$$

Plots of dielectric constant, dielectric loss, and $\tan\delta$ versus voltage of ZnO/n–Si device are shown in Figs. 4(a)–4(c), respectively for frequency changing from 10 kHz to 1 MHz. There are two peaks at low frequencies which are corresponding to depletion and accumulation regions but at high frequencies, only one peak appears with increasing frequency in Fig. 4(a). While the first peak can be attributed to the particular density distribution of N_{ss}, the second peak can be attributed to R_s and interfacial layer. It can be seen from this figure that the values of ε' and ε'' are a strong function of voltage and frequency at higher and intermediate bias voltage but they remain almost constant at low bias voltages (inversion region). The values of ε' and ε'' decrease with increasing frequency, which is attributed to the fact they cannot follow AC signal at high frequency because there is no so long time to orient the direction of the AC signal.[31] In other words, low values of ε' and ε'' are the results of the polarization processes and surface states and both of them decrease with increasing frequency since N_{ss} cannot follow an AC signal sufficiently at high frequencies. ε' and ε'' each reach a constant value at high frequencies (which can be seen in Fig. 1).[32]

The plots of tangent loss ($\tan\delta$) versus voltage of Au/ZnO/n–Si device shows that $\tan\delta$ increases with increasing frequency as indicated in Fig. 4(c). It can be seen from this figure that there are no changes at forward bias or in depletion and accumulation regions, but at reverse bias $\tan\delta$ values increase with increasing frequency up to 400 kHz then decrease to 1-MHz frequency. These changes of $\tan\delta$ value can be attributed to the changes of polarization at AC signals.[30]

The plots of dielectric constant, dielectric loss, and $\tan\delta$ versus frequency of ZnO/n–Si device for different voltages are shown in Figs. 5(a)–5(c), respectively for different voltages changing from 1 V to 2 V in steps of 0.25 V. As shown in these figures, the values of ε' and ε'' (the inset shows closer views in Fig. 5(b)) both decrease with increasing frequency and voltage, which can be attributed to the R_s, N_{ss}, and thickness of interlayer ZnO.[33]

Plots of $\tan\delta$ versus frequency of Au/ZnO/n–Si device for different voltages are shown in Fig. 5(c). As shown in this figure, the value of $\tan\delta$ initial increases with increasing frequency for lower voltages then decreases with increasing frequency. This case can be attributed to the fact that the surface states and dipoles have no more time for orienting the direction of the AC electric field.[34] Furthermore, $\tan\delta$ values decrease from depletion regions to accumulation regions with increasing voltage.

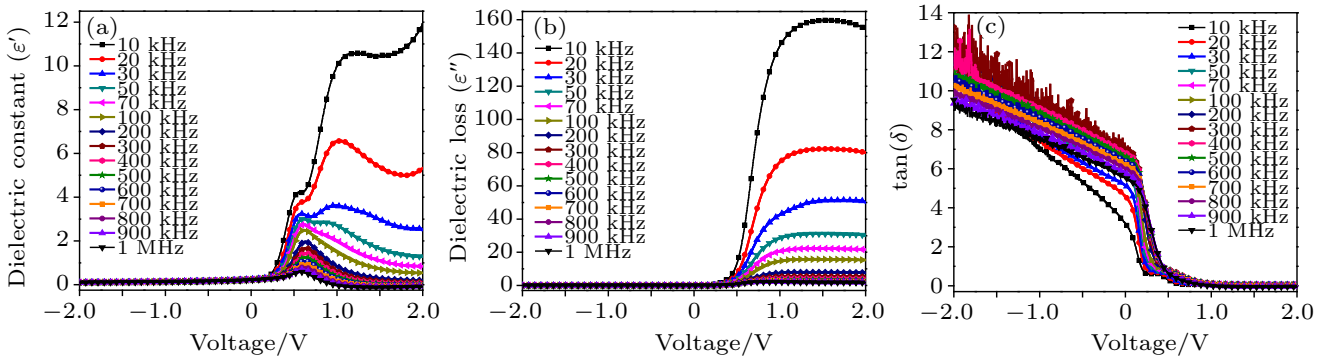


Fig. 4. (color online) Plots of (a) dielectric constant, (b) dielectric loss, and (c) tan δ versus voltage of Au/ZnO/n–Si device.

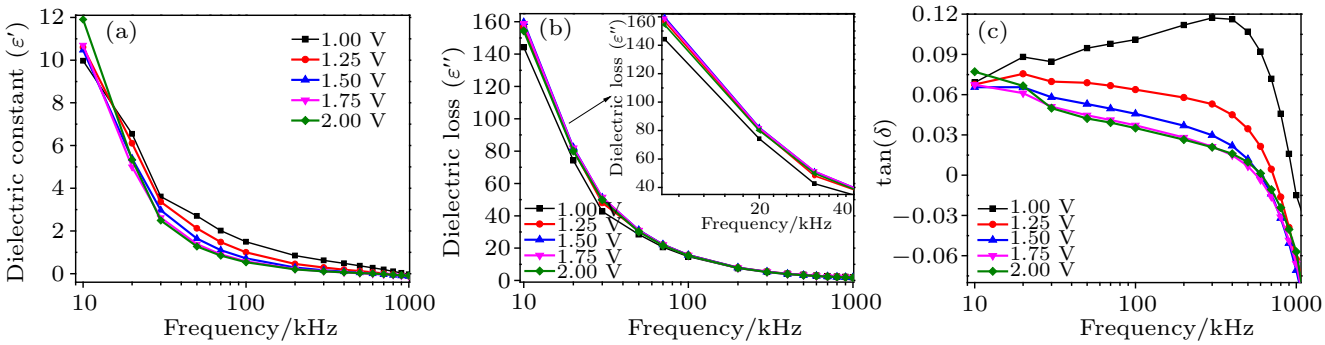


Fig. 5. (color online) Plots of (a) dielectric constant, (b) dielectric loss, and (c) tan δ versus frequency of Au/ZnO/n–Si device.

The complex dielectric constant ($\varepsilon^* = 1/M^*$) data are changed into the complex electric modulus formula ($M^* = M' + \mathrm{j}M''$) by using the following equation to find real and imaginary electric modulus:[24]

$$M^* = \frac{1}{\varepsilon^*} = \frac{\varepsilon'}{\varepsilon'^2 + \varepsilon''^2} + \mathrm{j}\frac{\varepsilon''}{\varepsilon'^2 + \varepsilon''^2} = M' + \mathrm{j}M''. \qquad (9)$$

The values of M' and M'' of the device are found to be strong functions of voltage and frequency. As shown in Fig. 6(a), the value of M' increases with increasing frequency in inversion and depletion regions but it becomes independent of frequency especially in the accumulation region. Figure 6(b) shows that M''–V plots have peaks and the positions of these peaks shift towards the accumulation region with increasing frequency. These conclusions could be attributed to the particular distribution of the charges in the surface states and their relaxation times.[10]

The plots of values of M' and M'' versus frequency of device are shown in Figs. 7(a) and 7(b) for different low bias voltages, respectively. It can be seen from these figures that the values of M' decrease with increasing biases because of removal electrode polarization, and the peaks are located at about 500-kHz frequency. Intensities of these peaks decrease with voltage increasing from 1 V to 2 V, which is attributed to a frequency-dependent dielectric relaxation.[31] M'' values, which indicates that the energy loss of device decreases with increasing voltage.

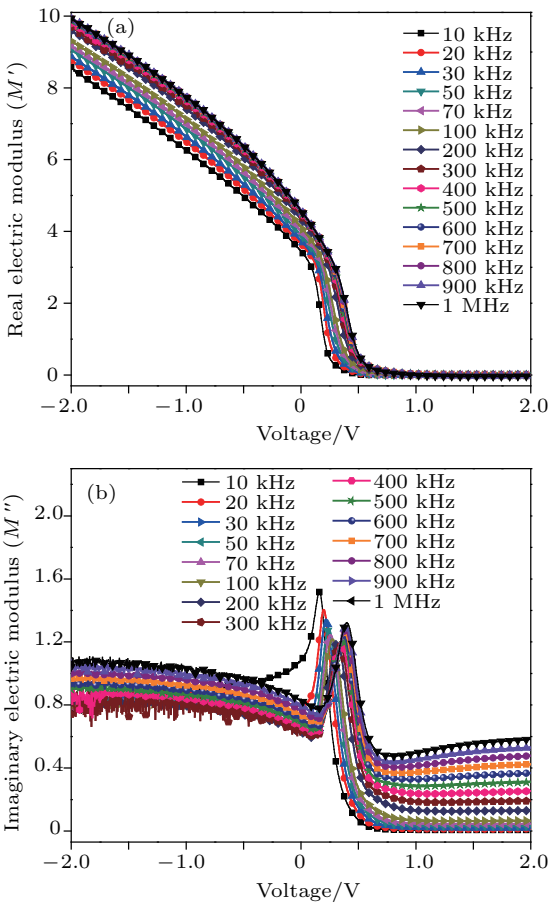


Fig. 6. (color online) Plots of (a) real and (b) imaginary electric modulus versus voltage of Al/ZnO/n–Si device at different frequency values.

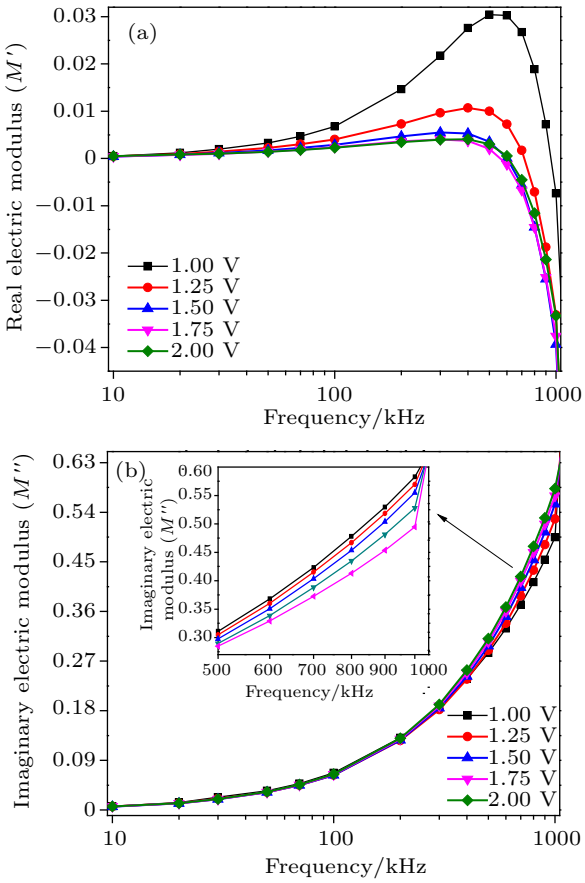


Fig. 7. (color online) Plots of (a) real and (b) imaginary electric modulus versus frequency of Au/ZnO/n–Si device at different voltages.

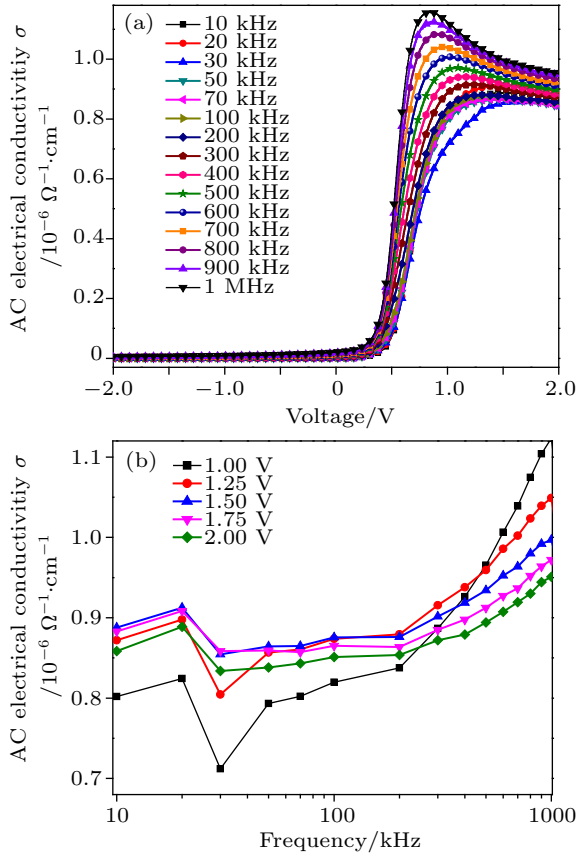


Fig. 8. (color online) Plots of AC electric conductivity versus (a) voltage at different frequency and (b) frequency at different voltages of Au/ZnO/n–Si device.

The value of AC electric conductivity (σ) can be calculated from the following equation:

$$\sigma = \left(\frac{d}{A}\right)\omega C \tan\delta = \varepsilon'' \omega \varepsilon_0. \tag{10}$$

The AC electric conductivity changing with voltage at different frequencies and changing with frequency at different voltages of Au/ZnO/n–Si device are shown in Figs. 8(a) and 8(b), respectively. As can be seen in Fig. 8(a), all σ–V plots have peaks at different frequencies in accumulation regions and increase with increasing frequency, positions of peaks shift towards high forward bias. In Fig. 8(b), AC electric conductivity is enhanced with increasing frequency and voltage. This increase in σ leads to the increase of eddy current which in turn increases the energy $\tan\delta$.[35] This increase in $\tan\delta$ can be attributed to reducing the series resistance and polarizations.[24,34,36,37]

4. Conclusions

The effects of surface states with various lifetimes and polarization processes on the electrical and dielectric characterizations of Au/ZnO/n–Si device is investigated, and both forward and reverse bias capacitance/conductance-voltage-frequency (C/G–V–f) measurements are performed in a frequency range of 10 kHz–1 MHz and at voltages of ± 2 V, respectively, at room temperature. On the other hand, the Au/ZnO/n-type Si device obtained by using ALD technique is studied at points of N_{ss}, R_s, BH, and N_d changing with frequency or voltage. The dielectric characterization and AC electric conductivity are also studied as functions of frequency and voltage. The values of ε', ε'', $\tan\delta$, M', M'', and σ are used in these characterizations with changing voltage and frequency. These characterizations show that all these physical parameters strongly depend on the frequency and voltage. While the values of ε' and ε'' decrease with increasing frequency, $\tan\delta$ increases up to 300 kHz then decreases for each forward bias voltage. M' and M'' values increase with increasing frequency, and in the case of M'', it is seen that the peaks and positions of these peaks shift with increasing frequency in the forward bias region. The value of σ increases with increasing voltage and frequency, which depends on reducing polarization and R_s. Consequently, it can be concluded that interfacial polarization and N_{ss} can easily follow an external AC signal especially at low frequencies.

References

[1] Kabra V, Aamir L and Malik M M 2014 *Beilstein J. Nanotechnol.* **5** 2216
[2] Jin W, Zhang K, Gao Z, Li Y, Yao L, Wang Y and Dai L 2015 *ACS Appl. Mater. Interfaces* **7** 13131
[3] Tatar B, Bulgurcuoğlu A E, Gökdemir P, Aydoğan P, Yilmazer D, Özdemir O and Kutlu K 2009 *Int. J. Hydrogen Energy* **34** 5208
[4] Sharma G D, Sharma S K and Roy M S 2004 *Thin Solid Films* **468** 208

[5] Ren N, Sheng K, Zhang J M and Peng F Z 2013 *IEEE Energy Conversion Congress and Exposition* (IEEE) p. 2871

[6] Chen L, Deng J, Gao H, Yang Q, Wang G, Kong L, Cui M and Zhang Z 2016 *J. Mater. Sci. Mater. Electron.* **27** 4275

[7] Yadav A B, Pandey A, Somvanshi D and Jit S 2015 *IEEE Trans. Electron Devices* **62** 1879

[8] Orak İ, Ejderha K and Turut A 2015 *Curr. Appl. Phys.* **15** 1054

[9] Gümüş A, Ersöz G, Yücedağ İ, Bayrakdar S and Altindal Ş 2015 *J. Korean Phys. Soc.* **67** 889

[10] Kaya A, Alialy S, Demirezen S, Balbaşı M, Yerişkin S A and Aytimur A 2016 *Ceram. Int.* **42** 3322

[11] Rajan L, Periasamy C and Sahula V 2016 *IEEE Trans. Nanotechnol.* **15** 201

[12] Pradel K C, Jevasuwan W, Suwardy J, Bando Y, Fukata N and Wang Z L 2016 *Chem. Phys. Lett.* **658** 158

[13] Marimuthu T, Anandhan N, Thangamuthu R, Mummoorthi M and Ravi G 2016 *J. Alloys Compd.* **677** 211

[14] Su Y Q, Zhu Y, Yong D, Chen M, Su L, Chen A, Wu Y, Pan B and Tang Z 2016 *J. Phys. Chem. Lett.* **7** 1484

[15] Li X B, Zhang X, Li L C, Huang L L, Zhang W, Ye J D and Hong J G 2016 *Mater. Lett.* **175** 122

[16] Zhang Z L, Zheng G, Qu F Y and Wu X 2012 *Chin. Phys. B* **21** 098104

[17] Ameen S, Park D-R, Shaheer Akhtar M and Shin H S 2016 *Mater. Lett.* **164** 562

[18] Boujnah M, Boumdyan M, Naji S, Benyoussef A, El Kenz A and Loulidi M 2016 *J. Alloys Compd.* **671** 560

[19] Liu C Y, Xu H Y, Sun Y, Ma J G and Liu Y C 2014 *Opt. Express* **22** 16731

[20] He J, Cheng C and Hu J 2016 *AIP Adv.* **6** 30701

[21] Singh S K, Hazra P, Tripathi S and Chakrabarti P 2016 *Superlattices Microstruct.* **91** 62

[22] Park Y J, Song H, Ko K B, Ryu B D, Cuong T V and Hong C H 2016 *J. Nanomater.* **2016** 1

[23] Şafak-Asar Y, Asar T, Altındal Ş and Özçelik S 2015 *J. Alloys Compd.* **628** 442

[24] Demirezen S 2013 *Appl. Phys. A* **112** 8273

[25] Tanrıkulu E E, Yıldız D E, Günen A and Altındal Ş 2015 *Phys. Scr.* **90** 95801

[26] Cherif A, Jomni S, Mliki N and Beji L 2013 *Physica B: Condens. Matter* **429** 79

[27] Yücedağ İ, Kaya A, Altındal Ş and Uslu I 2014 *Chin. Phys. B* **23** 047304

[28] Zeyrek S, Acaroğlu E, Altındal Ş, Birdoğan S and Bülbül M M 2013 *Curr. Appl. Phys.* **13** 1225

[29] Nicollian E H and Brews J R 2003 *MOS (metal oxide semiconductor) physics and technology* (Wiley-Interscience)

[30] Sze S M 1981 *Physics of Semiconductor Devices* (Newyork: Wiley)

[31] Ataseven T, Tataroglu A, Memmedli T and Özçelik S 2012 *J. Optoelectron. Adv. Mater.* **14** 640

[32] Yıldız D E and Dökme I 2011 *J. Appl. Phys.* **110** 14507

[33] Yücedağ İ, Ersöz G, Gümüş A and Altındal Ş 2015 *Int. J. Mod. Phys. B* **29** 1550075

[34] Kaya A, Altındal Ş, Asar Y Ş and Sönmez Z 2013 *Chin. Phys. Lett.* **30** 017301

[35] Bülbül M M 2007 *Microelectron. Eng.* **84** 124

[36] Altındal Yerişkin S, Balbaşı M and Tataroğlu A 2016 *J. Appl. Polym. Sci.* **133**

[37] Baraz N, Yücedağ İ, Azizian-Kalandaragh Y and Altındal Ş 2016 *J. Mater. Sci.: Mater. Electron.* 1–7